Supporting Information

Rolland et al. 10.1073/pnas.1303872110

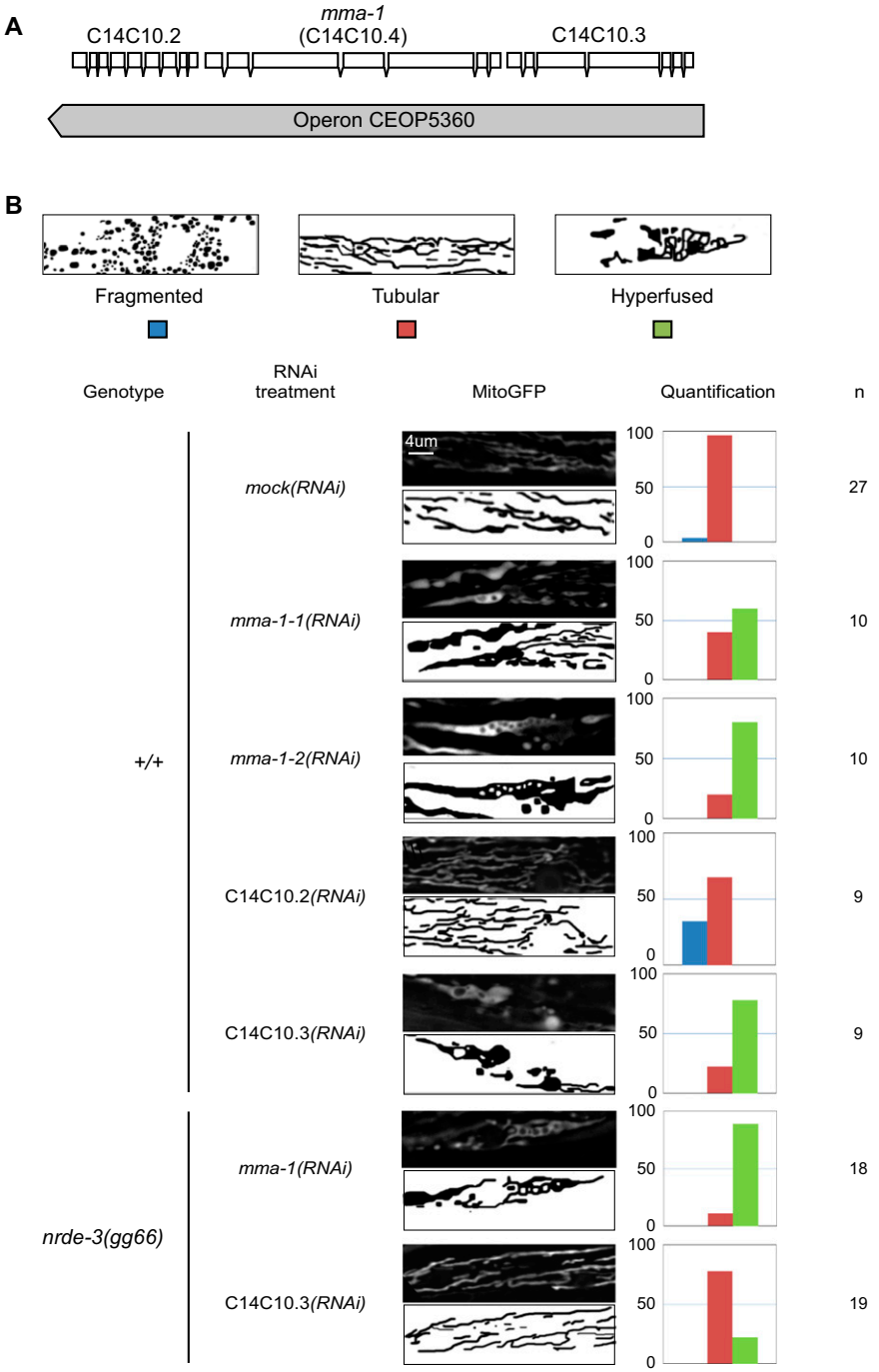

Fig. S1. Mitochondrial morphology abnormal-1(RNAi) [*mma-1(RNAi)*] causes mitochondrial hyperfusion. (*A*) The CEOP5360 operon, containing C14C10.2, *mma-1*, and C14C10.3 is indicated. (*B*) MD3011 [*bcIs78* (*Pmyo-3:mitoGFP*)] or MD3098 [*bcIs78*(*Pmyo-3:mitoGFP*);*nrde-3*(*gg66*)] L4 larvae were treated with *mma-1–1(RNAi)*, *mma-1-2(RNAi)*, C14C10.2*(RNAi)*, or C14C10.3*(RNAi)* and mitochondrial morphology in body-wall muscle cells of L4 *larvae* of the F1 generation was analyzed by fluorescent microscopy [*mma-1–1(RNAi)* and *mma-1–2(RNAi)* are two RNAi constructs directed against the 5′ and 3′ of the *mma-1* ORF, respectively]. MitoGFP images and schematic of the representative mitochondrial morphology observed in each condition are shown. The frequencies of the different categories of mitochondrial morphology observed as well as the number of animals analyzed are indicated (*n*).

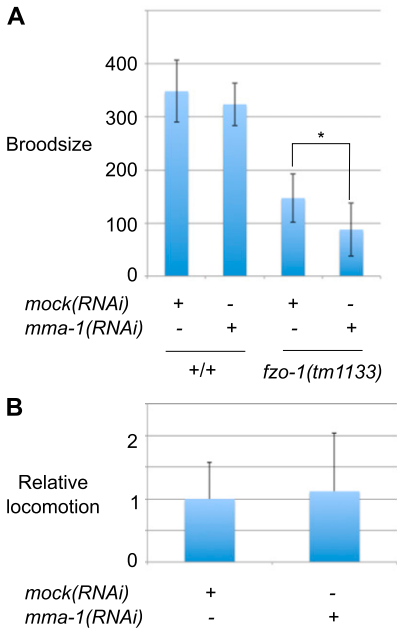

Fig. S2. *mma-1(RNAi)* effect on broodsize and locomotion. (*A*) The broodsize of 10 animals of each genotype was analyzed. (*$P = 0.047$ by Student *t* test). (*B*) The number of body bends per minute for 15 animals of each genotype was measured. The value indicated are standardized to the *mock(RNAi)* control (SD is indicated). The differences were not statistically significant ($P = 0.78$).

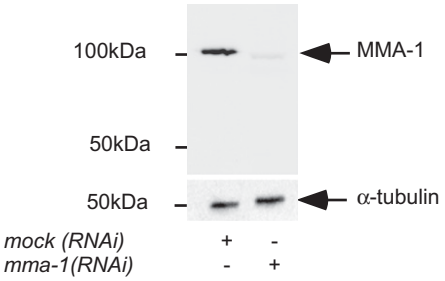

Fig. S3. Rabbit polyclonal anti–MMA-1 antibodies recognize specifically the MMA-1 protein. Mixed-stage worm protein extracts from *mock(RNAi)* or *mma-1* (*RNAi*) worms analyzed by Western analysis using affinity-purified rabbit polyclonal anti–MMA-1 antibodies.

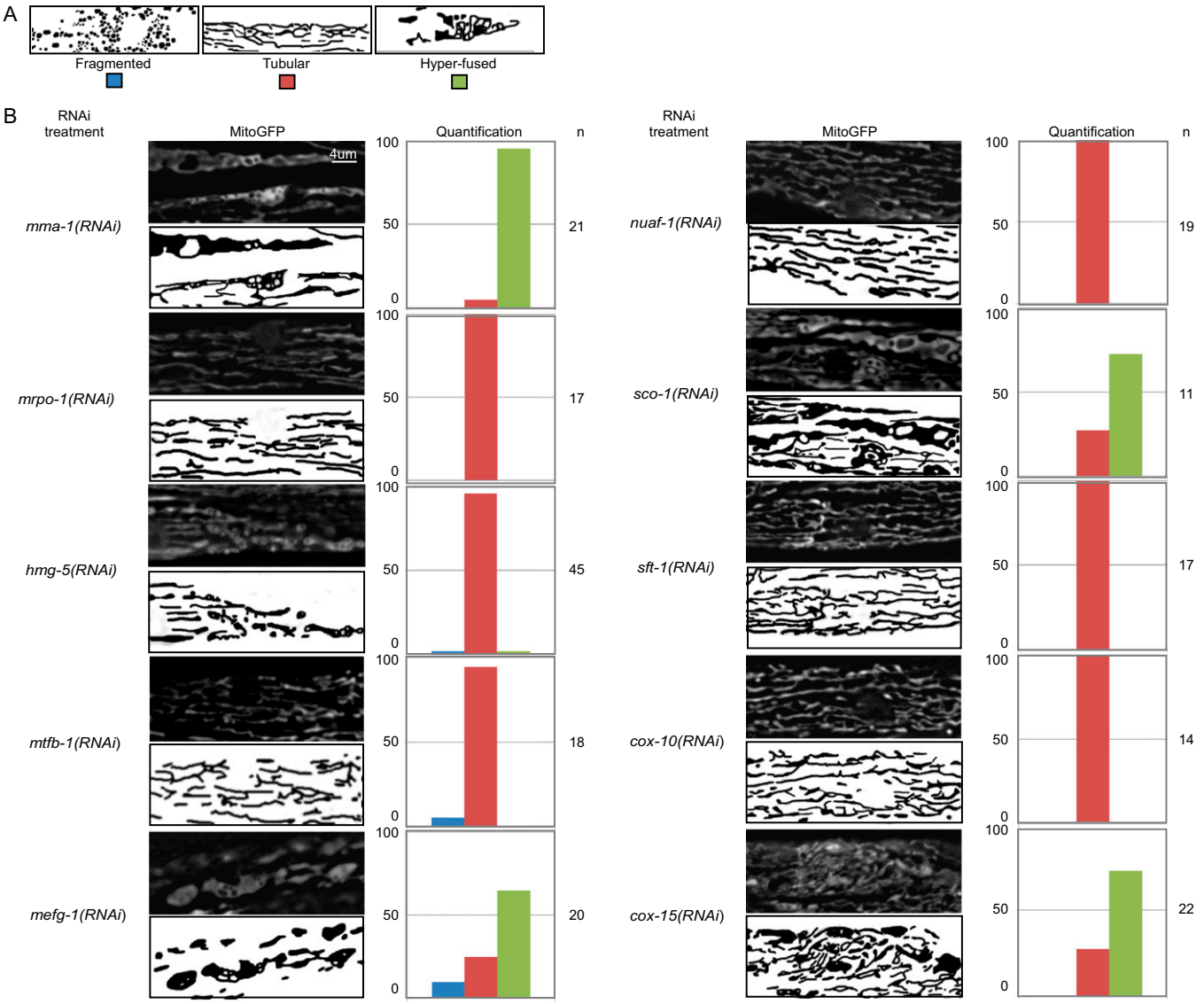

Fig. S4. Inactivation of various genes by double-strand RNA (dsRNA) injection and its effect on mitochondrial morphology. MD3011 [*bcIs78* (*Pmyo-3:mitoGFP*)] adults were injected with the corresponding dsRNA and mitochondrial morphology in body-wall muscle cells of L4 *larvae* of the F1 generation was analyzed by fluorescent microscopy. (*A*) Schematic of the different mitochondrial morphologies observed. (*B*) MitoGFP images and schematic of the representative mitochondrial morphology observed in each condition are shown. The frequencies of the different categories of mitochondrial morphology observed as well as the number of animals analyzed are indicated (*n*).

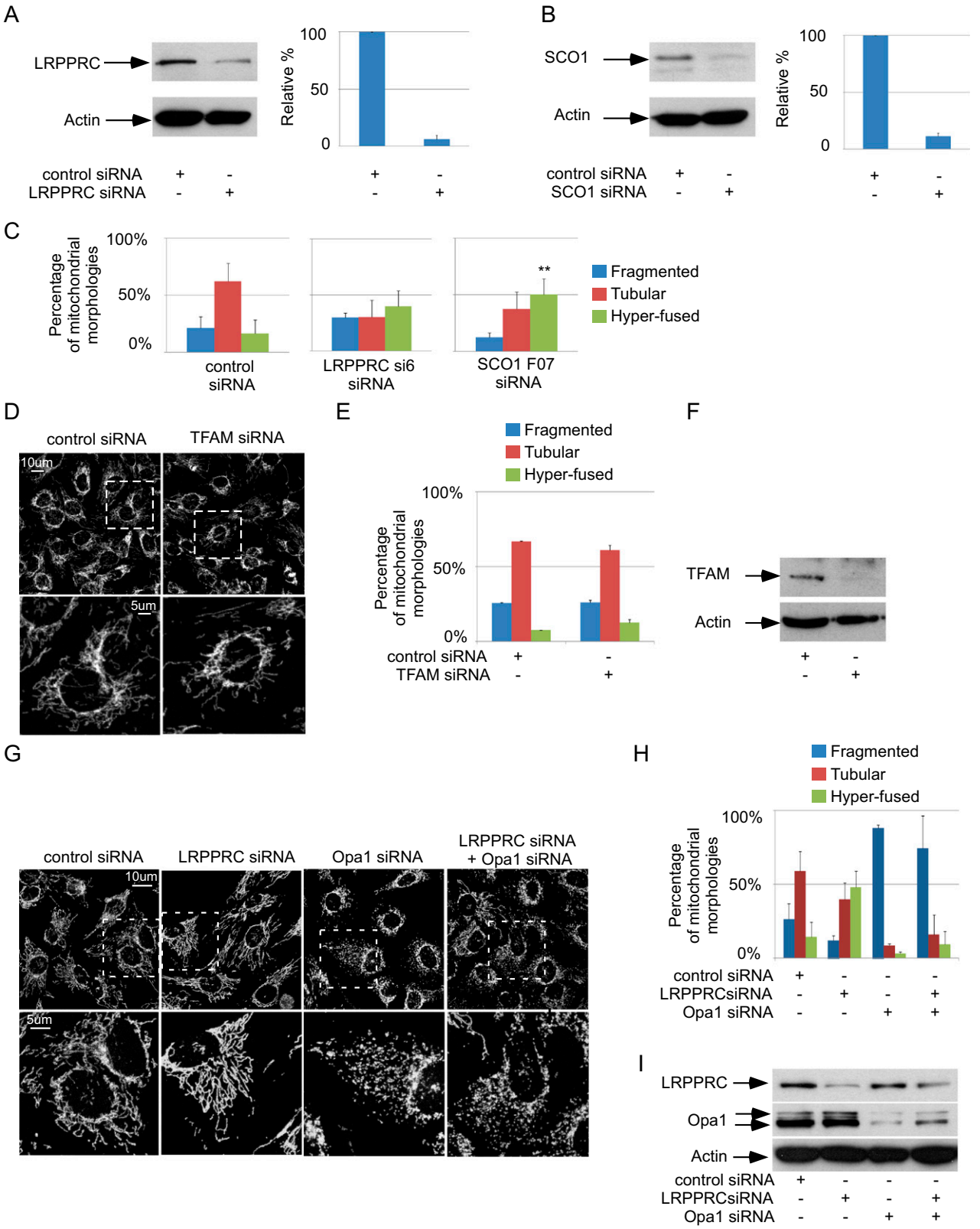

Fig. S5. Inactivation of the LRPPRC (leucine-rich pentatricopeptide repeat containing) but not transcripton factor A mitochondrial (TFAM) cause mitochondrial hyperfusion. (*A*) Efficiency of LRPPRC siRNA shown in Fig. 6 assessed by Western analysis ($n = 3$). (*B*) Efficiency of SCO1 siRNA shown in Fig. 6 assessed by Western analysis ($n = 2$). (*C*) Effect of two different siRNA against LRPPRC or SCO1 ($n > 3$). The double asterisks (**) represent the difference between the number of hyperfused mitochondrial upon SCO1 siRNA and control siRNA is significant by Bonferroni's multiple comparison test ($P < 0.01$). (*D*) Mitochondria of SH-SY5Y cells treated for 3 d with mock or TFAM siRNA were visualized using anti-Tom20 antibodies. Maximum projections of a representative *z*-stack for each condition as well as an enlargement are shown. (*E*) Quantifications of the different mitochondrial morphologies were made in two independent experiments (SDs are indicated). (*F*) Efficiency of TFAM siRNA assessed by Western analysis. (*G*) Mitochondria of SH-SY5Y cells treated for 3 d with control siRNA, Opa1

Legend continued on following page

siRNA, LRPPRC siRNA, or Opa1 siRNA and LRPPRC siRNA were visualized using anti-Tom20 antibodies. Maximum projections of a representative *z*-stack for each condition as well as an enlargement are shown. (*H*) Quantifications of the different mitochondrial morphologies were made in three independent experiments (SDs are indicated). (*I*) Efficiency of LRPPRC and Opa1 siRNA assessed by Western analysis.

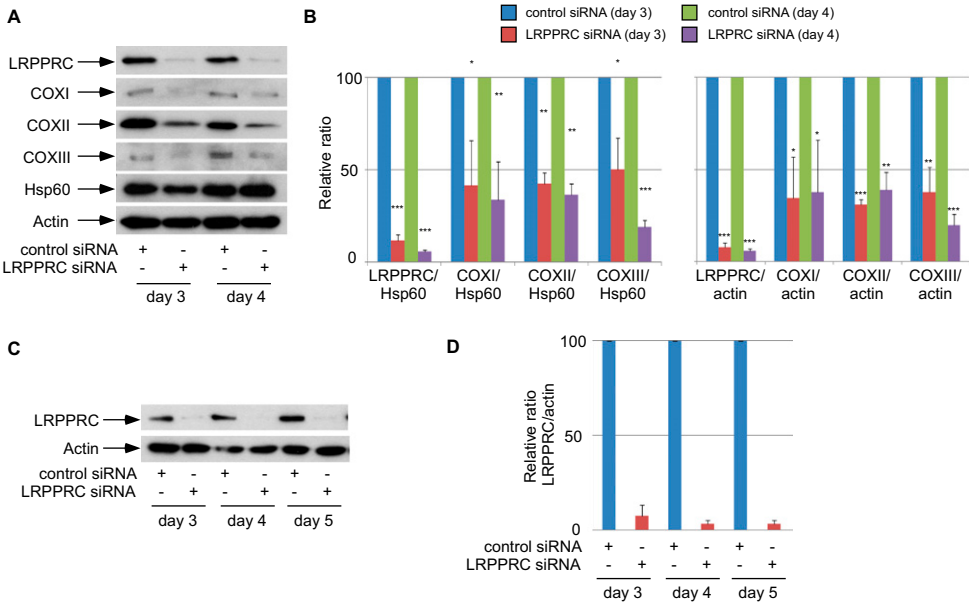

Fig. S6. Analysis of the effect of LRPPRC siRNA on different mitochondrial proteins (*A*) Western analyses of COXI, COXII, COXIII, LRPPRC, Hsp60, and actin after control siRNA or LRPPRC siRNA. (*B*) Quantifications were performed out of three independent experiments. The difference between each experimental siRNA and its corresponding control siRNA were analyzed by Student *t* test (**P* < 0.05, ***P* < 0.01, and ****P* < 0.001). (*C*) Western analyses of LRPRRC and Actin protein levels after control siRNA or LRPPRC siRNA for 3, 4, and 5 d. (*D*) Quantifications were performed out of at least two independent experiments for each time point.

Table S1. Strains, genotypes, and transgenes

Strain	Genotype	Transgene
MD3011	*bcIs78* I	*Pmyo-3:mitoGFP* (pVDB#1* at 5 ng/μL)
MD2963	*bcIs78* I;*fzo-1*(*tm1133*) II	*Pmyo-3:mitoGFP* (pVDB#1* at 5 ng/μL)
MD3000	*bcIs78* I;*drp-1(tm1108)* IV	*Pmyo-3:mitoGFP* (pVDB#1* at 5 ng/μL)
MD3099	*bcIs78* I;*eat-3(tm1107)* II	*Pmyo-3:mitoGFP* (pVDB#1* at 5 ng/μL)
MD3098	*bcIs78* I;*nrde-3(gg66)* X	*Pmyo-3:mitoGFP* (pVDB#1* at 5 ng/μL)
MD2922	*bcEx856*	*Pmyo-3:PAmitogfp* (pBC900 at 2 ng/μL) and *Pmyo-3:mitodsred* (pBC914) (0.2 ng/μL) and pRF4 at 80 ng/μL

*Kind gift from A. van der Bliek (University of California, Los Angeles, CA).

Table S2. RNAi strains used for RNAi by feeding

RNAi strains	Description
mma-1(*RNAi*)	*mma-1* (*RNAi*) strain from Ahringer library (1)
mma-1–1(*RNAi*)	*mma-1* fragment (nt297-503) from *mma-1* cDNA cloned into NcoI site of pPD129.36
mma-1–2(*RNAi*)	*mma-1* fragment (nt2652-2874) from *mma-1* cDNA cloned into NcoI site of pPD129.36
fzo-1(*RNAi*)	*fzo-1*(*RNAi*) strain from Ahringer library
drp-1(*RNAi*)	*drp-1*(*RNAi*) strain from Ahringer library
C14C10.2(*RNAi*)	*C14C10.2*(*RNAi*) strain from Ahringer library
C14C10.3(*RNAi*)	*C14C10.3*(*RNAi*) strain from Ahringer library
gfm-1(*RNAi*)	*gfm-1*(*RNAi*) strain from Ahringer library. *Caenorhabditis elegans* ortholog of mitochondrial translation elongation factor G1 EFG1
nuaf-1(*RNAi*)	*nuaf-1*(*RNAi*) strain from Ahringer library. *C. elegans* ortholog of the complex I assembly factor NDUAF1
sco-1(*RNAi*)	*sco-1*(*RNAi*) strain from Ahringer library. *C. elegans* ortholog of the complex IV assembly factor SCO1

1. Kamath RS, Ahringer J (2003) Genome-wide RNAi screening in *Caenorhabditis elegans*. *Methods* 30(4):313–321.

Table S3. Plasmids used to generate dsRNA for RNAi by injection

Plasmid	Insert	Target
pBC1088	*mma-1* fragment (nt297-503)	*mma-1*
pBC1181	*tfbm-1* entire cDNA	*C. elegans* ortholog of the mitochondrial transcription factor TFB1M
pBC1188	*hmg-5* exon 2	*C. elegans* ortholog of the mitochondrial transcription factor TFAM
pBC1208	*rpom-1* exon 3	*C. elegans* ortholog of the mitochondrial RNA polymerase POLMRT
pBC1209	*gfm-1* exon 3	*C. elegans* ortholog of the mitochondrial translation elongation factor G1, EFG1.
pBC1213	*nuaf-1* exon 5	*C. elegans* ortholog of the complex I assembly factor, NDUAF1.
pBC1214	*sco-1* exon 2	*C. elegans* ortholog of the complex IV assembly factor, SCO1.
pBC1210	*sft-1* exon 2	*C. elegans* ortholog of the complex IV assembly factor, SURF1.
pBC1211	*cox-10* exon 7	*C. elegans* ortholog of the complex IV assembly factor, COX10.
pBC1212	*cox-15* exon 3	*C. elegans* ortholog of the complex IV assembly factor, COX15.

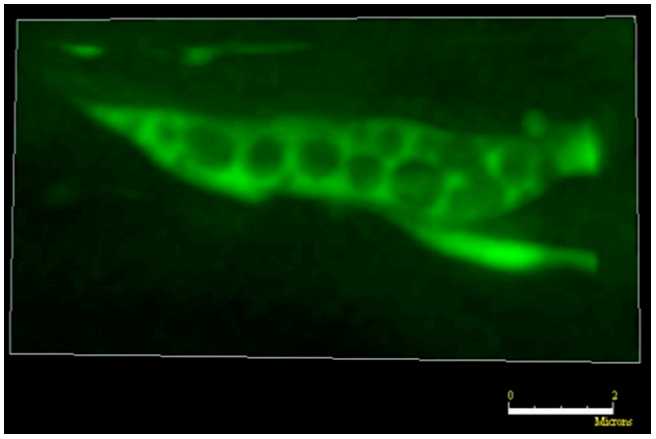

Movie S1. *mma-1(RNAi)* causes mitochondrial hyperfusion (related to Fig. 1). A *z* stack taken on an epifluorescent microscope of a representative muscle cell of MD3011 animal treated with *mma-1(RNAi)* was used to generate a 3D reconstruction using AutoDeblur/AutoVisualize software. The video represents a ±45° rotation of the 3D reconstruction. mitoGFP-labeled mitochondria are shown in green.

Movie S1